

# EFFECT OF LOADING RATE AND GEOMETRY ON FLEXURAL BEHAVIOUR OF TEXTILE REINFORCED CONCRETE

NERSWN BASUMATARY\*, ROSHINI RAMANATHAN<sup>†</sup> AND KEERTHANA KIRUPAKARAN<sup>+</sup>

<sup>\*†</sup>Department of Civil Engineering  
Indian Institute of Technology Madras (IITM), Chennai, India

\*e-mail: nerswnb.civil@gmail.com

<sup>†</sup>e-mail: roshiniramanathan14@gmail.com

<sup>+</sup>e-mail: keerthanak@civil.iitm.ac.in

**Key words:** Textile Reinforced Concrete, Loading Rate, Geometry size, Fracture Energy

**Abstract:** Mechanical and fracture behaviour of Textile Reinforced Concrete (TRC) depends on several factors such as the type of textile fibre, number of textile layers, cement matrix strength, volume fraction of fibres, mesh size, aggregate size, and most importantly the bonding between the textile fibre and the matrix. In this study, the flexural behaviour of TRC panels under monotonic loading is investigated by varying loading rates and geometrical parameters. The experiments are conducted on TRC panels containing four layers of E-glass textile fibre reinforcement under a three-point bending configuration. The effect of specimen size and rate of loading is analyzed by considering two sizes of TRC panels of dimensions 100 × 200 × 35 mm (S12) and 200 × 400 × 35 mm (S24) subjected to rates of loading of 0.5 mm/min, 1 mm/min, and 2 mm/min. Further, the Digital Image Correlation (DIC) technique is used to investigate the fracture behaviour of TRC panels. The mechanical and fracture characteristics such as load-displacement curves, first-crack load, post-peak flexural behaviour, and fracture energy are evaluated, and a comparison is drawn for TRC specimens of different geometrical sizes subjected to different rates of loading.

## 1 INTRODUCTION

Textile Reinforced Concrete (TRC) is a new-generation fibre-cement composite material that has better sustainable potential than traditional reinforced concrete and a much lower CO<sub>2</sub> footprint [1-2]. TRC replaces the use of steel reinforcement by using 2D or 3D textile fibres as continuous reinforcements. Different types of fibres such as basalt fibre, alkali-resistant glass, polypropylene, and carbon fibres have been used in TRC. The concrete cover of TRC is thin and therefore it is possible to produce thin and light structural components with excellent bearing capacity and ductility. Currently, the main application of TRC is in the form of facades construction and strengthening

of existing concrete structures. Since there is no steel reinforcement in TRC, it is corrosion free and has potential applications in the construction of marine structures, stormwater drains, sewage tanks, and catchment basins [3-4]. For structural applications of TRC, assessment of its mechanical performance is essential. Several researchers have studied the direct tensile behaviour of TRC by using different setups. Under uniaxial tension, the TRC exhibits trilinear behaviour, which can be characterized into three zones. Zone I corresponds to the elastic stage dominated by the matrix, zone II corresponds to the multiple-cracking stage, and zone III corresponds to the post-multiple-cracking stage, which is

dominated by the properties of textiles [5-6]. Zargarán et al. [7] categorized the typical behaviour of TRC under flexural loading into two zones as shown in Figure 1. The first zone is dominated by the role of concrete where the concrete matrix breaks, and a sudden drop occurs (part a – part b). Following the drop (part b), the concrete cracks begin to widen, and depending on the volume fraction of the textile reinforcement, the curve shows a deflection hardening or under-reinforced response (part c).

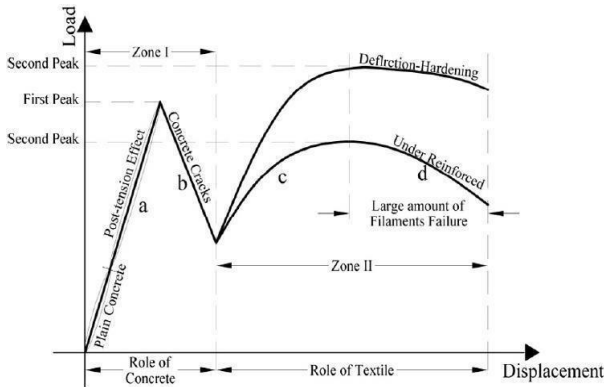


**Figure 1:** Typical behaviour of TRC under flexural load [7]

Unlike conventional concrete, two types of bonds must be considered while understanding the bonding behaviour of TRC: the bond between filaments and concrete; and the bond between the filaments themselves [8-9]. Portal et al., [10], performed an experiment to study the pull-out behaviour of TRC with basalt and carbon textile reinforcement and reported that the bond between the filaments and the concrete matrix is subject to some deficiencies. Hegger et al. [3] performed a four-point bending test to study the flexural behaviour of TRC reinforced with textiles made of carbon and alkali-resistant (AR) glass fibres and reported that the increase in the reinforcement ratio led to the higher elongation of the flexural strength because of the smaller crack spacing. Du et al. [11], reported that the flexural strength and toughness of basalt textile-reinforced concrete (BTRC) specimens improved with an increase in the number of textile layers. Zargarán et al. [12] emphasized that the mesh size and the number of TRC layers greatly influence the

failure characteristics in TRC. They reported that using a maximum grain size of 2 mm in a fibre spacing of less than 5 mm mesh size was not viable for easy penetration of concrete matrix between the fibres. Silva et al. [13] conducted three-point bending tests to investigate the cementitious composites reinforced with unidirectional continuous sisal fibres and reported a reduction in flexural stiffness due to the formation of cracks. Tsesarsky et al. [14] performed three-point bending tests on TRC reinforced with three different types of textile fibres. Their findings revealed distinct behaviours for each type: the polyethylene (PE) TRC exhibited high ductility despite its low strength, the AR glass TRC showed intermediate strength but demonstrated brittle behaviour, while the carbon TRC showcased both high flexural strength and ductility.

Literature on the mechanical performance of TRC predominantly focuses on its tensile behaviour and there are few works reported on its flexural behaviour. Since the properties of TRC are influenced by different geometric and loading parameters, this paper focuses on the flexural behaviour of TRC panels reinforced with four layers of E-glass fibres. In this work, E-glass fibre is chosen due to its low cost compared to AR-glass textile fibre. TRC panels are subjected to monotonic loading under three-point bending by varying loading rates and geometrical parameters. The paper is structured as follows: Section 2 describes the experimental program, Section 3 and Section 4 elaborates on the experimental results, and finally, the conclusions are discussed in Section 5.

## 2 EXPERIMENTAL PROGRAM

### 2.1 TRC panel specimen preparation

#### 2.1.1 Concrete Mix

The mixture proportion of concrete consists of Ordinary Portland Cement (OPC), blended with fly ash and micro silica. The matrix composition is summarized in Table 1. A Polycarboxylate Ether (PCE) superplasticizer of 0.15% by weight of the binder is used in the mix. The maximum size of the aggregate of 1.2

mm is used to ensure easy penetration of the aggregates through the grid size of the textile. The 28 days cube compressive strength and split-cylinder tensile strength of concrete were obtained as 50 MPa and 4.5 MPa respectively. The modulus of elasticity was computed according to ASTM-C469 [15] standard as 30 GPa. The mechanical property of concrete is summarized in Table 2.

**Table 1:** Concrete mix design details

Materials	Values
Cement(kg/m <sup>3</sup> )	: 583
Fly ash (kg/m <sup>3</sup> )	: 208
Silica fume (kg/m <sup>3</sup> )	: 42
Quartz sand (kg/m <sup>3</sup> )	: 595
Quartz powder (kg/m <sup>3</sup> )	: 357
Water/binder	: 0.4
Maximum size of aggregate (mm)	: 1.2
PCE superplasticizer (% solids/binder by weight)	: 0.15

**Table 2:** Mechanical properties of concrete

28-day compressive strength	: 50 MPa
28-day tensile strength (MPa)	: 4.5 MPa
28-day flexural strength (MPa)	: 6.9 MPa
Modulus of Elasticity	: 30 GPa
Age of the specimen	: 1.5 Years

### 2.1.2 Textile reinforcement

A leno weave E-glass textile fiber as shown in Figure 2 is embedded in the concrete mortar to make TRC. The schematic of the leno weave is shown in Figure 3. The properties of the textile reinforcement are given in Table 3. The textile has a nominal tensile strength of 1650 MPa and a modulus of elasticity of 70 MPa as per the manufacturer. The mesh opening size of the textile reinforcement is 16 × 16 mm. The textile reinforcement was manually pulled from either side to induce prestress. This pre-tension force restricts sagging and helps in proper

alignment while placing the textile fibre in the concrete mortar. A large panel of size 3 × 1.5 m was initially cast and then the required panel size was cut from this bigger panel. In this study, TRC panels of size 100 × 200 × 35 mm and 200 × 400 × 35 mm are used.

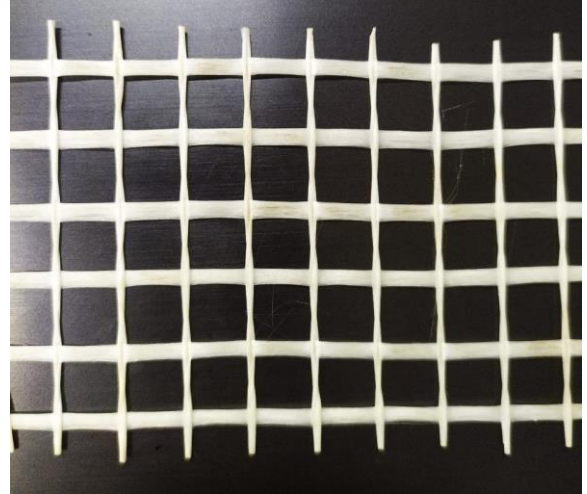


**Figure 2:** Leno weave E-glass textile fibre

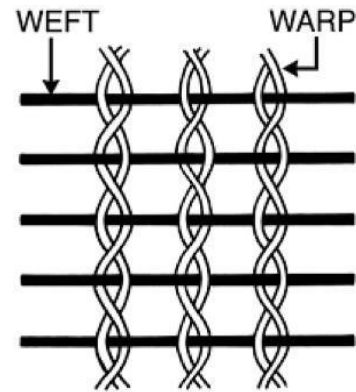


**Figure 3:** Schematic of leno weave textile fibre [16]

**Table 3:** Properties of textile reinforcement

Type of fibre	: E-glass
No. of textile layers	: 4
Diameter of Textile	: 0.9 mm
Type of weaving	: Leno weave
Grid size	: 16 × 16 mm
Volume fraction of fibre	: 0.91%
Modulus of elasticity	: 70MPa

## 2.2 Experimental test set-up

### 2.2.1 Three-point bending test

The flexural test of the TRC specimen was performed in a three-point bending configuration according to the ASTM E72 standard [17] and the experimental set-up is shown in Figure 4. A clear span of 150 mm and 350 mm is considered for the specimen size of  $100 \times 200 \times 35$  mm (S12) and  $200 \times 400 \times 35$  mm (S24) respectively. Material Testing Systems (MTS) with closed loop servo-hydraulic machine of 100-tonne load cell is used for testing the TRC panels. The TRC panels of two sizes (S12 and S24) were subjected to three loading rates: 0.5 mm/min, 1 mm/min, and 2 mm/min. The Linear Variable Differential Transformer (LVDT) is placed in the bottom face of the TRC panel to obtain vertical deflection under three-point bending. The data acquisition rate of 10 Hz is used to record the data which includes time, load, actuator displacement, and vertical displacement from LVDT. To understand the fracture characteristics in the TRC panel, Digital Image Correlation (DIC) technique is used, which is described in the following

section.

### 2.2.2 Digital Image Correlation (DIC) set-up

Digital Image Correlation (DIC) is a non-contact and non-destructive optical measurement technique used to assess surface displacement and strain in a deforming body. The DIC set-up is shown in Figure 5. To perform DIC analysis, the specimen surface is prepared by applying a black speckle pattern using spray paint. Then a series of digital images are captured as the specimen undergoes deformation. By employing a correlation algorithm, the displacements and stresses on the specimen's surface are analyzed by tracking the movement of pixels in the digital photographs taken in both the undamaged and deformed states. For capturing digital photos, a 12.3 Megapixel resolution camera is used, which is securely fixed to tripod support, and positioned such that its axis remains parallel to the plane of the deforming specimen. The photos were captured at a rate of 10 photos per second. The DIC analysis is performed using Istra 4D image processing software from Dantec Dynamics [18].

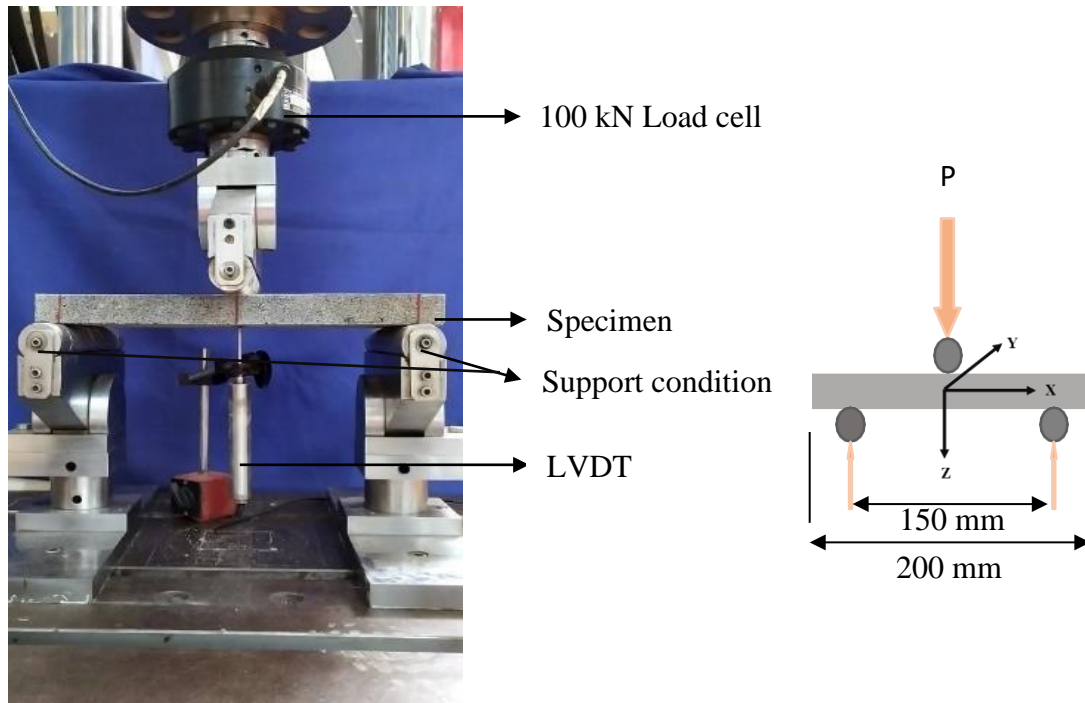


**Figure 4:** Experimental set-up of three-point bending test

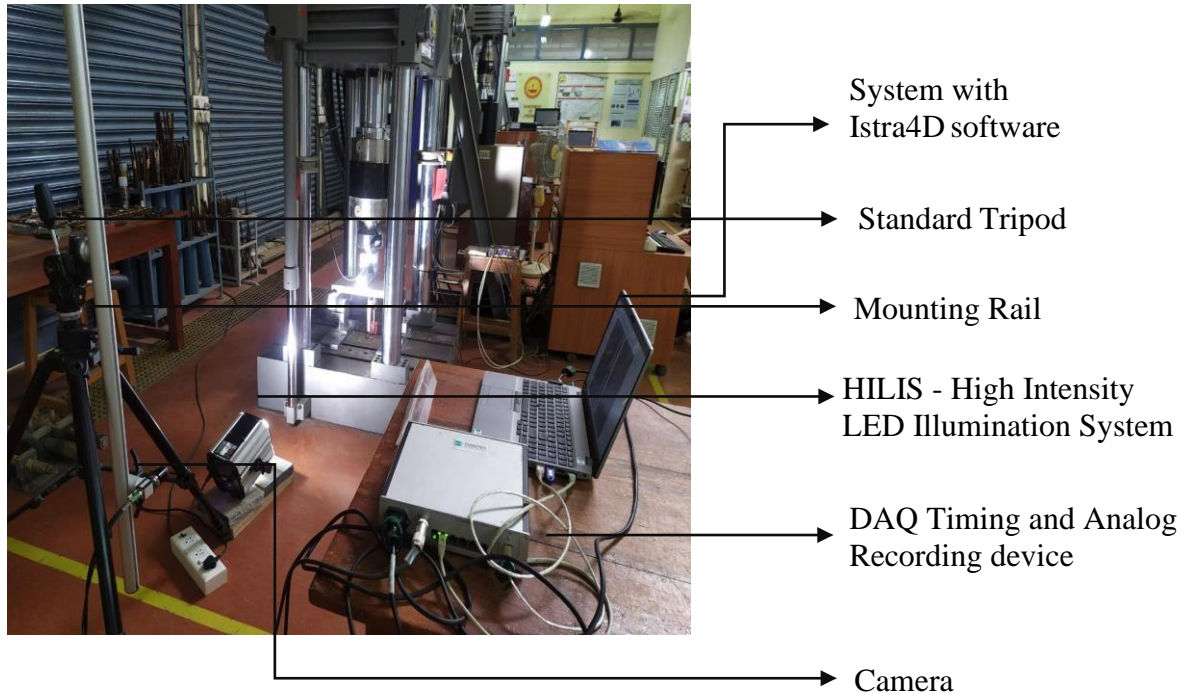


Figure 5: Experimental set-up for Digital Image correlation (DIC)

### 3 MECHANICAL TEST RESULTS

#### 3.1 Typical behaviour of TRC panel

The typical load-deflection response of the TRC panel tested under three-point bending is depicted in Figure 6. The load-deflection curve can be divided into four zones: Zone 1 from O-A, Zone 2 from A-B, Zone 3 from B-C, and Zone 4 from C-D as shown in Figure 6. The first zone from O to A, is an elastic zone with point A indicating the first crack load in the concrete mortar matrix. Beyond point A, microcracks in concrete occur and softening is observed till point B. Between points B and C, strain hardening occurs due to the composite action of TRC. Beyond point C, the textile fails through rupture, and gradual softening is observed until the failure at point D. All the specimen irrespective of different sizes showed this typical trend. However, the variation amongst the specimens is observed due to the tortuosity of the crack pattern and the heterogeneous nature of the TRC composite. The variation of load-deflection curves of three specimens of size S24 is shown in Figure 7, where the shaded region indicates the maximum and minimum

bound of the variation and the solid black line indicates the average. A similar flexural trend has been reported in the literature [6-7] as well. However, the strain hardening response in zone 3 can vary based on the volume fraction of textile fabric used. In this study, the volume fraction of 0.91% is kept constant for all the specimens irrespective of change in the specimen dimension. The effect of loading rate and specimen dimension in concrete is discussed in the following sections.

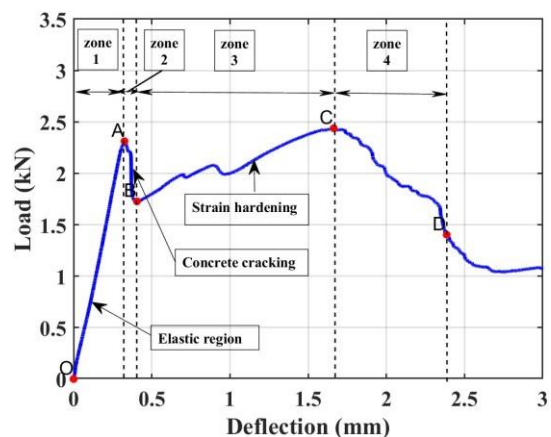
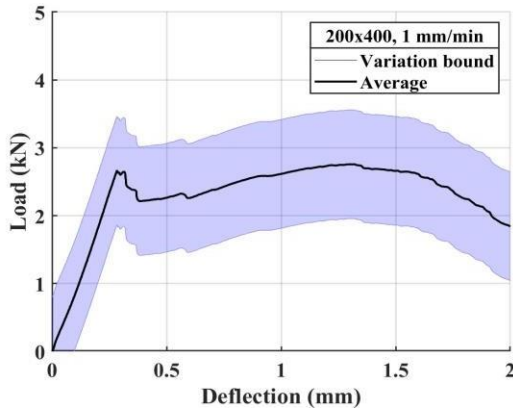


Figure 6: Typical behaviour of TRC under flexure



**Figure 7:** Flexural response of TRC panel with the variation bound

### 3.2 Effect of loading rate

A three-point bending test was performed under three loading rates: 0.5 mm/min, 1 mm/min, and 2 mm/min on specimens of dimensions  $100 \times 200 \times 35$  mm (S12) and  $200 \times 400 \times 35$  mm (S24). The comparison of the load-deflection curve under different loading rates is shown in Figure 8 and Figure 9 for S12 and S24 specimens respectively. The typical trend under flexure is observed in all the specimens (S12 and S24). The variation between the specimens for a particular loading rate is attributed to the heterogeneous composition of the material. As these are unnotched specimens the crack initiates in the mid-zone between the supports and based on the tortuosity of the crack pattern the load-deformation response shows variation. Figures 10 (a) and (b) show the variation in the load corresponding to points A, B, C, and D in S12 and S24 specimens respectively. The following observation is made from these Figures.

- For S12 specimens, the variation of average load at point A decreases with an increase in the loading rate, however, a reverse trend is observed for S24 specimens. This anomaly can be attributed to specimen heterogeneity.

- At other points, B, C, and D in both S12 and S24, the load increases with an increase in the rate of loading.

- The difference in the increase in load at points B, C, and D is large for the loading rate

of 0.5 mm/min compared to the 1 and 2 mm/min rate of loading.

These observations illustrate that the effect of loading rate is prominent for lower loading rates such as 0.5 mm/min and below, particularly after the first crack load (point A).

### 3.3 Effect of specimen dimension

The comparison of the load-deflection values at various points: A, B, C, and D in the curve for both the specimen sizes S12 and S24 at a loading rate of 0.5 mm/min, 1 mm/min, and 2 mm/min is shown in Table 4. The comparison of load values at various points for two sizes of specimens (S12 and S24) subjected to loading rates 0.5, 1, and 2 mm/min are shown in Figures 11 (a), (b) and (c) respectively. The difference in the first crack load at point A is prominent between S12 and S24 for a loading rate of 0.5 and 1 mm/min. At other points (B, C, and D), the effect of specimen dimension is not very significant. However, from Table 4, it is observed that the deflection values at various points are higher in S24 specimens compared to smaller specimen S12. These observations indicate that the larger size of the specimen in the X-Y plane tends to give a larger deflection. However, the thickness (Z-direction) of the TRC panel can significantly influence the TRC behaviour under flexure.

## 4 FRACTURE CHARACTERIZATION OF TRC PANEL

As TRC flexural response shows four distinct zones it is important to understand fracture behaviour in these zones and to characterize fracture properties such as fracture energy. In this study, Digital Image Correlation (DIC) is used to quantify the fracture properties of TRC which is elaborated in the following section.

### 4.1 Interpretation of DIC results

Digital Image Correlation (DIC) system is used to analyze the surface crack propagation. The DIC results for S24 specimens subjected to a rate of loading 0.5 and 1 mm/min are shown in Figures 12 and 13 respectively. The surface

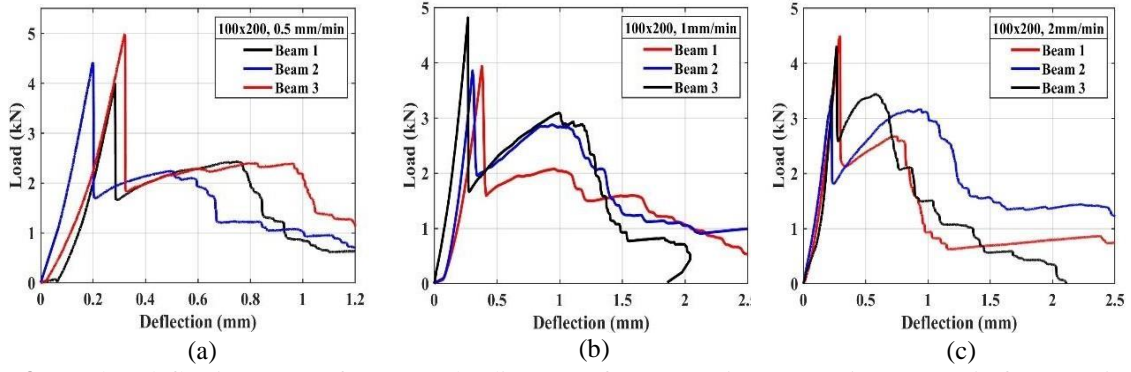


**Figure 8:** Load vs deflection curve of TRC at a loading rate of 0.5 mm/min, 1 mm/min, 2 mm/min for a specimen size 100 mm x 200 mm x 35 mm

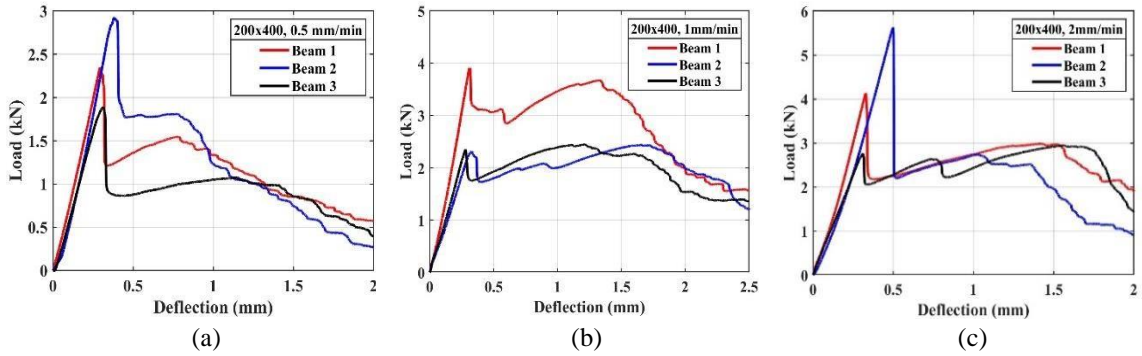


**Figure 9:** Load vs deflection curve of TRC at a loading rate of 0.5 mm/min, 1 mm/min, 2 mm/min for a specimen size 200 mm x 400 mm x 35 mm

**Table 4:** Load-deflection values at various points

Loading rate (mm/min)	specimen	A		B		C		D	
		LVDT (mm)	Load (kN)						
0.5	S12	0.26	4.47	0.28	1.72	0.74	2.35	0.94	1.17
1	S12	0.17	4.20	0.22	1.74	0.84	2.68	2.9	2.7
2	S12	0.18	3.56	0.21	1.99	1	2.92	3.38	3.01
0.5	S24	0.32	2.39	0.39	1.28	0.92	1.45	1.44	0.85
1	S24	0.21	2.85	0.36	2.10	1.31	2.87	4.67	3.02
2	S24	0.25	4.67	0.37	2.15	1.10	2.80	4.63	2.30

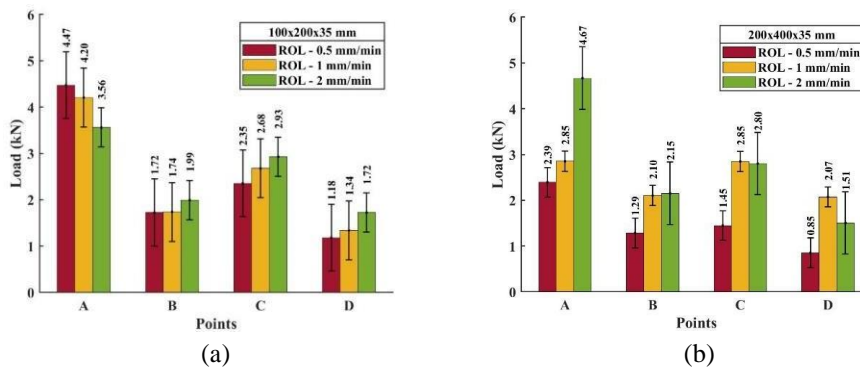


**Figure 10:** Comparison of mean load vs mean deflection at various points at a varying loading rate for (a) S12 and (b) S24 specimens

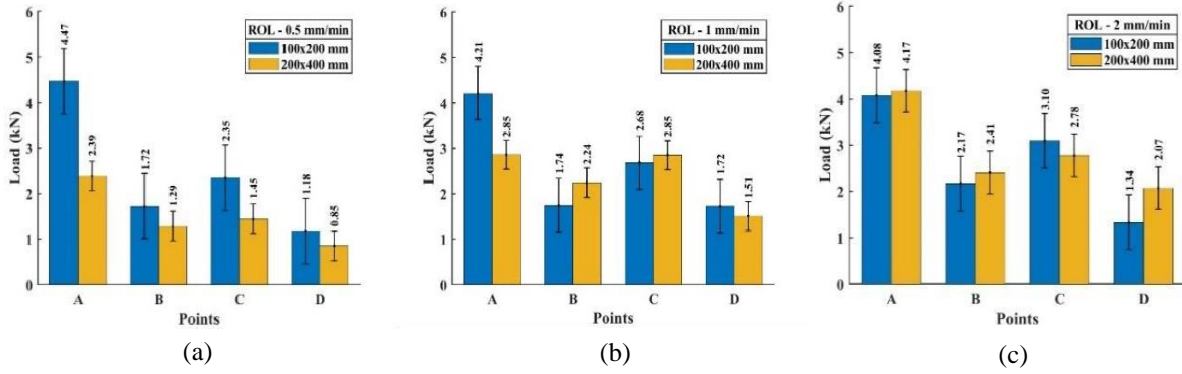


Figure 11: Comparison of geometry size S12 and S24 at loading rates: (a) 0.5 mm/min (b) 1 mm/min (c) 2 mm/min

crack pattern along the depth at points A, B, C, and D are shown in these figures. For specimen S24 at 0.5 mm/min loading rate, the crack is observed at points A and B but for S24 at 1 mm/min loading rate the crack at these points is not prominently visible. However, from point C, the crack is prominently visible on the S24 specimen subjected to a loading rate of 1 mm/min. Between points C and D, the crack propagates and widens as the load is transferred from the concrete matrix to the textile fibre reinforcement. The crack width is calculated from DIC and is plotted against the load in Figure 14. It can be seen that the load-crack

width follows the same trend as that of the load-deflection curve. The bonding between the textile fibres and the concrete matrix should be such that the failure of the specimen should not occur due to the slip rather it should fail in rupture [9]. In this work, the failure of all the specimens occurred due to the rupture of the textile fibre. Thus, it delays the failure and contributes to the ductile behaviour of TRC. Therefore, it can be inferred that increasing the number of textile layers with improved bonding strength can significantly improve the ductility and residual load-carrying capacity of TRC.

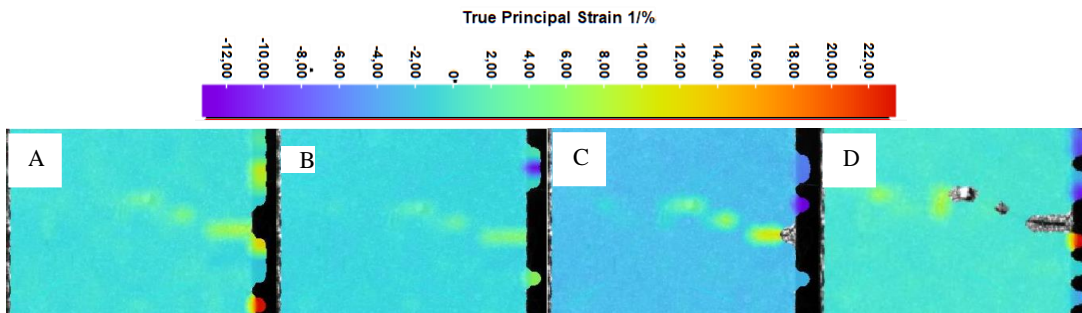


Figure 12: Crack penetration and propagation pattern across the depth of specimen S24 at various points at a loading rate of 0.5 mm/min

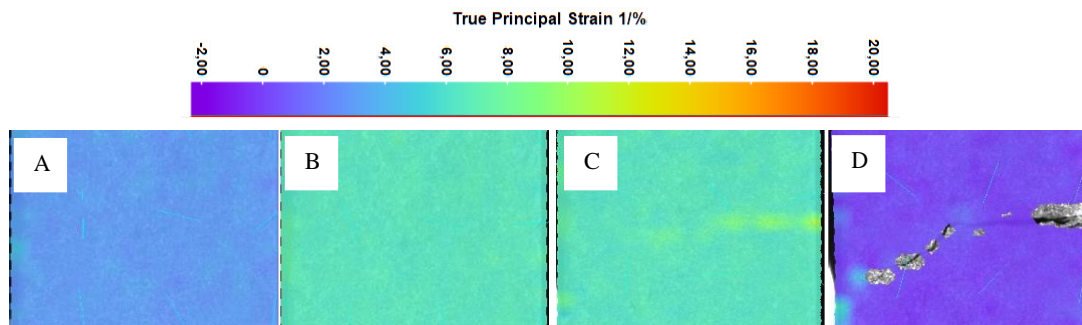


Figure 13: Crack penetration and propagation pattern across the depth of specimen S24 at various points at a loading rate of 1 mm/min

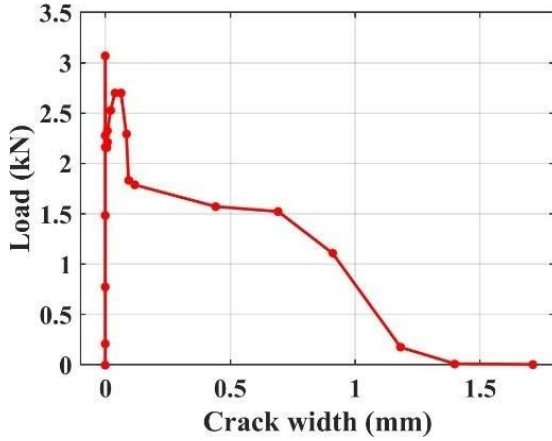


Figure 14: Crack width across the depth of the specimen

Table 5: Total crack width and crack length

Loading rate (mm/min)	Specimen	Crack width (mm)	Crack length (mm)
0.5	S24	1.56	37
1	S24	1.67	36
2	S24	1.71	37

#### 4.2 Fracture energy of TRC Panels

Fracture energy refers to the energy released by the material per unit crack area. In this work, the fracture energy of TRC panels is calculated considering the area under the load-deflection curve up to point D. Unlike beam specimens, there was a challenge in computing the fracture

energy due to significant crack tortuosity along the X-Y plane. Figure 15 shows the crack pattern along the panel depth (X-Z plane) and width (X-Y plane) of the specimen. The surface crack length along the depth (X-Z plane) and width (X-Y plane) on either side of the specimen is measured by placing a thread along the path of the crack and the average crack length along these two planes is taken to calculate the fracture surface area. The fracture energy is determined by dividing the area under the load-deflection curve up to point D by the fracture surface area which is tabulated in Table 6. It is observed that while the difference in fracture energy at the loading rates of 1 mm/min and 2 mm/min is not prominent, the fracture energy was considerably higher when compared to the loading rate of 0.5 mm/min in both the specimen size (S12 and S24).

Table 6: Fracture energy

Loading rate (mm/min)	Specimen	Mean Gf (N/mm)	Std dev. Gf (N/mm)
0.5	S12	0.48	0.10
1	S12	0.73	0.20
2	S12	0.75	0.13
0.5	S24	0.34	0.05
1	S24	0.66	0.17
2	S24	0.68	0.06



Figure 15: Crack propagation and failure pattern of specimens

### 5 SUMMARY AND CONCLUSIONS

In this research, the behaviour of TRC under flexural loading conditions, the effect of load loading rate and geometry size, and the characterization of macro crack are experimentally investigated. The experiment has been carried out in three-point bending with the aid of Digital Image Correlation (DIC).

The important conclusions drawn from this experiment are:

- (1) The effect of loading rate in load-deflection response is prominent at a lower loading rate of 0.5 mm/min as compared to a higher loading rate of 1 mm/min to 2 mm/min in both the sizes of the specimen.
- (2) The larger the size of the specimen along the X-Y plane tends to give a larger deflection.

(3) Digital Image Correlation (DIC) system is used to quantify the fracture properties and surface crack propagation.

(4) The fracture energy increases with the increase in the loading rate, with the increase being prominent when the higher loading rates (1mm/min and 2 mm/min) are compared to the loading rate of 0.5 mm/min.

## 6 ACKNOWLEDGEMENTS

The authors wish to thank the staff, researchers, and professors of the Building Technology and Construction Management (BTCM), Department of Civil Engineering, IITM, Chennai, India. The help of research scholars, Mr. Ramakrishna S and Mr. Sachin Paul is highly appreciated. The support through the Institute of Eminence Research Initiative Grant on Technologies for Low Carbon and Lean Construction from IIT Madras is acknowledged.

## REFERENCES

- [1] Hegger, J., Curbach, M., Stark, A., Wilhelm, S., & Farwig, K. (2018). Innovative design concepts: Application of textile reinforced concrete to shell structures. *Structural Concrete*, 19(3), 637-646.
- [2] Tomoscheit, S., Gries, T., Horstmann, M. and Hegger, J., 2011. Project life INSUSHELL: Reducing the carbon footprint in concrete construction. *International Journal of Sustainable Building Technology and Urban Development*, 2(2), pp.162-169.
- [3] Hegger, J., & Voss, S. (2008). Investigations on the bearing behaviour and application potential of textile reinforced concrete. *Engineering structures*, 30(7), 2050-2056.
- [4] Yin, S. P., Li, Y., Jin, Z. Y., & Li, P. H. (2018). Interfacial Properties of Textile-Reinforced Concrete and Concrete in Chloride Freezing-and-Thawing Cycle. *ACI Materials Journal*, 115(2).
- [5] Tysmans, T., Adriaenssens, S., Cuypers, H. and Wastiels, J., 2009. Structural analysis of small-span textile reinforced concrete shells with double curvature. *Composites science and technology*, 69(11-12), pp.1790-1796.
- [6] Li, B., Xiong, H., Jiang, J. and Dou, X., 2019. Tensile behavior of basalt textile grid reinforced Engineering Cementitious Composite. *Composites Part B: Engineering*, 156, pp.185-200.
- [7] Zargaran, M., Attari, N.K., Alizadeh, S. and Teymouri, P., 2017. Minimum reinforcement ratio in TRC panels for deflection hardening flexural performance. *Construction and Building Materials*, 137, pp.459-469.
- [8] Soranakom, C. and Mobasher, B., 2009. Geometrical and mechanical aspects of fabric bonding and pullout in cement composites. *Materials and structures*, 42, pp.765-777.
- [9] Yang, J.M., Lee, J. and Chang, C., 2023. Effect of Reinforcement Ratio and Bond Characteristic on Flexural Behavior of Carbon Textile-Reinforced Concrete Panels. *Materials*, 16(10), p.3703.
- [10] Portal, N.W., Perez, I.F., Thrane, L.N. and Lundgren, K., 2014. Pull-out of textile reinforcement in concrete. *Construction and Building Materials*, 71, pp.63-71.
- [11] Du, Y., Zhang, X., Zhou, F., Zhu, D., Zhang, M. and Pan, W., 2018. Flexural behavior of basalt textile-reinforced concrete. *Construction and Building Materials*, 183, pp.7-21.
- [12] Zargaran, M., Attari, N.K. and Alizadeh, S., 2022. Flexural behavior of high-performance and non-high-performance textile reinforced concrete composites. *European Journal of Environmental and*

*Civil Engineering*, pp.1-15.

- [13] de Andrade Silva, F., Zhu, D., Mobasher, B. and Toledo Filho, R.D., 2011. Impact behavior of sisal fiber cement composites under flexural load. *ACI materials journal*, 108(2), p.168.
- [14] Tsesarsky, M., Peled, A., Katz, A. and Anteby, I., 2013. Strengthening concrete elements by confinement within textile reinforced concrete (TRC) shells—Static and impact properties. *Construction and Building Materials*, 44, pp.514-523.
- [15] Yildirim, H. and Sengul, O., 2011. Modulus of elasticity of substandard and normal concretes. *Construction and building materials*, 25(4), pp.1645-1652.
- [16] Shaker, K., Nawab, Y., Ayub Asghar, M., Nasreen, A. and Jabbar, M., 2020. Tailoring the properties of leno woven fabrics by varying the structure. *Mechanics of Advanced Materials and Structures*, 27(22), pp.1865-1872.
- [17] ASTM Committee E-6 on Performance of Buildings, 2005. *Standard test methods of conducting strength tests of panels for building construction*. ASTM International.
- [18] <https://www.dantecdynamics.com/solutions/digital-image-correlation-dic/>